Design, construction and performance of UVES, the echelle spectrograph for the UT2 Kueyen telescope at the ESO Paranal Observatory

H. Dekker, S. D'Odorico, A. Kaufer, B. Delabre and H. Kotzlowski
European Southern Observatory
Karl-Schwarzschildstr. 2, D85748 Garching, Germany

ABSTRACT

We describe the design and construction of the ESO UV-Visual Echelle Spectrograph and the performance that was measured during its commissioning in 1999. UVES is a dual-beam, grating crossdispersed echelle spectrograph. The resolution for a 1 arcsecond slit is 40 000. With narrower slits, resolutions of up to 80 000 (blue) and 115 000 (red arm) are achieved with adequate sampling. UVES provides order separations of minimum 10 arcseconds at any wavelength between 320 and 1050 nm. The wavelength coverage is 100 nm in the blue arm and 200 or 400 nm in the red arm, with possibility to use a dichroic. Some concepts pioneered in UVES are now increasingly being used in other echelle spectrographs for large telescopes: a white pupil design, very steep replicated mosaic echelles, and large refractive cameras with external focus. Regular observations are starting in April 2000 at the Nasmyth focus of Kueyen, Unit Telescope 2 of the VLT array.
Keywords: spectrograph design, echelle gratings, CCDs, dioptric cameras.

1. INTRODUCTION

UVES is a representative of a new class of high resolution spectrographs on 8-10 m class telescopes. The first example of these instruments is HIRES on the Keck telescope which has been an important reference point for the development of UVES. Other examples are HROS (Gemini), HRS (HET) and HDS (Subaru). These instruments probe into new domains of observational astrophysics and for the first time allow to investigate in detail the physics of galactic and extragalactic objects that were out of reach of 4-m class telescopes. A comparision of their technical concepts was made in 1995 by Pilachowski et al. [1]

Common to these instruments are new engineering challenges. In the absence of adaptive optics that will be out of reach for some time for at least the visible domain, high spectral resolution can only be attained using larger gratings, mechanics and optics. In our case, the need to efficiently use the costly investment of an 8-10 m telescope compelled us to use new concepts: a double beam white pupil spectrograph layout, use of steep mosaic (but monolithic) R4 echelles and dioptric cameras with high-efficiency coatings. Three state of the art CCD detectors were selected for optimum QE in the UV-blue, Visual and NIR.

TABLE 1. MILESTONES

04/92:	*Project kickoff*
04/94:	*Re-scope, resolution increased to 10^5, CCD mosaics, addition of ADC, I2 cell and other features*
1996	*Receipt of echelle mosaics*
1997	*Receipt of derotator, preslit optics, red camera and moving functions*
1998	*Receipt of collimator, table and enclosure*
09/98	*"First Light Europe": Solar spectrum*
02/99	*Receipt of blue camera and blue CCD*
05/99	*System test Europe completed*
12/99	*Commissioning completed*
02/00	*Science Verification*
04/00	*Release*

This paper concentrates on optomechanical design and on performance. The UVES CCDs are described in detail by Dorn et al.[2]. The paper by Longinotti et al.[3] at this conference describes the UVES control software within the VLT control and data flow system environment that is aimed at maximize the observing efficiency. The paper by Ballester et al.[4] addresses the data reduction and automatic assessment of data quality of UVES and other VLT instruments. Other information and instructions for prospective users can be found in the on-line User Manual[5] and on the UVES web page[6]. In the paper by D'Odorico given at this conference[7], the scientific capability of UVES as derived from the analysis of the data obtained during the commissioning is reported.

2. PROJECT OVERVIEW

Following extensive discussions in the ESO community where various concepts were explored, project kickoff for UVES was in 1992 with a plan[8] calling for two identical instruments, to go to the Nasmyth focii of UT2 and UT3, with a resolution of up to 70 000. In 1994, triggered by developments in the overall VLT Instrumentation Plan that reduced the emphasis on instrument

In *Optical and IR Telescope Instrumentation and Detectors*, Masanori Iye, Alan F. M. Moorwood, Editors, Proceedings of SPIE Vol. 4008 (2000) • 0277-786X/00/$15.00

duplication, it was decided to build a single instrument with increased spectral resolution and versatility [9]. The very fast (F/1.25) original design for the red camera for a 30 mm square field was replaced by an F/2.5 camera with twice the field size and much better sampling, allowing to exceed R = 10^5 in the red arm with a narrow (0.3") slit. This decision was facilitated by the appearance on the horizon of 2Kx4K CCD devices with low dark current and readout noise, while confidence grew that the VLT would indeed deliver the excellent image quality offered by the Paranal site. Other features that were included in the plan at this time were an Atmospheric Dispersion Compensator (ADC), Iodine Cell, Exposure Meters and an extra blue crossdisperser.

TABLE 2. MAJOR SUPPLIERS

SESO (F)	*Derotator prism, cameras, collimators and coatings*
Richardson Grating Laboratory (USA)	*Echelle mosaics, crossdispersers # 1 and # 3*
ELAN /Vavilov Institute (R)	*Crossdispersers # 2 and #4*
Schott (D), Ohara (F/J), Zeiss (D), Bicron (USA), APM/Aries (D/R)	*Optical glasses and single crystal CaF2*
Romabau (CH) and Kern (D)	*Table and enclosure, motorized functions*
WZW (CH)	*Image slicers*
G. Marcy (Lick, USA)	*Iodine Cell*
Barr (USA) and Balzers (FL)	*Dichroics*
Halle (D)	*Depolarizer and ADC prisms*
EEV Ltd. (GB) and MIT/LL (USA)	*CCD chips*
Cryodiffusion (F) and SARL (F)	*Cryogenic equipment*

In the new plan, the budget was decreased to 7.1 MDM, estimated manpower was 35 man-years and the commissioning was to take place from 7/99 to 12/99. These objectives were met, in the case of the budget with a small margin. The milestones in the UVES project have been summarized in Table 1.

UVES has been designed and assembled in-house as an ESO project. Major elements and subassemblies were contracted to industrial suppliers. Table 2 lists companies that contributed important parts. The instrument software has been developed in collaboration with the Astronomical Observatory of Trieste.

3. SCIENCE DRIVERS AND DESIGN CHOICES

The science objectives of UVES are listed in Table 3. We give them here to derive the four main drivers for the instrument design: *(1)* The need to *maximize the efficiency* led us to select a white-pupil layout and refractive cameras in two arms with optimized coatings, CCDs and crossdispersers; *(2) large wavelength coverage* to observe lines over a large spectral interval for QSO absorption line studies or abundance studies is achieved with large-area CCDs, a range of gratings with groove densities optimized to make the most efficient use of that area, and optional dichroics; *(3) sky subtraction capability* is essential since at the limiting magnitude of 19-20, the contribution from a dark sky is non-negligible. UVES competes with FORS2 and FLAMES on the same telescope; both are visible multi-object facilities with low- to medium spectral resolution, so it could be expected that a significant fraction of UVES observations would be scheduled for grey- or bright time. A large interorder space also permits to feed UVES with up to 8 fibers from the FLAMES facility[10] for multi-object work at R= 45 000, as well as to implement image slicers and *(4)* the radial velocity studies require *excellent wavelength accuracy* so UVES is mounted at the Nasmyth focus on a table inside a thermal enclosure for high mechanical and thermal stability.

TABLE 3. SCIENCE OBJECTIVES

- *Structure, physical conditions and abundances of interstellar and intergalactic gas at early epochs from the absorption spectra of high redshift QSO's*
- *Kinematics of gas and stars in galactic nuclei*
- *Kinematics and mass distributions of star clusters*
- *Composition, kinematics and physical conditions of the interstellar medium in the galaxy and in nearby systems*
- *Chemical composition and atmospheric models of galactic and extragalactic stars*
- *Substellar companions of nearby stars (high-precision radial velocity studies over long time scales)*
- *Stellar oscillations*

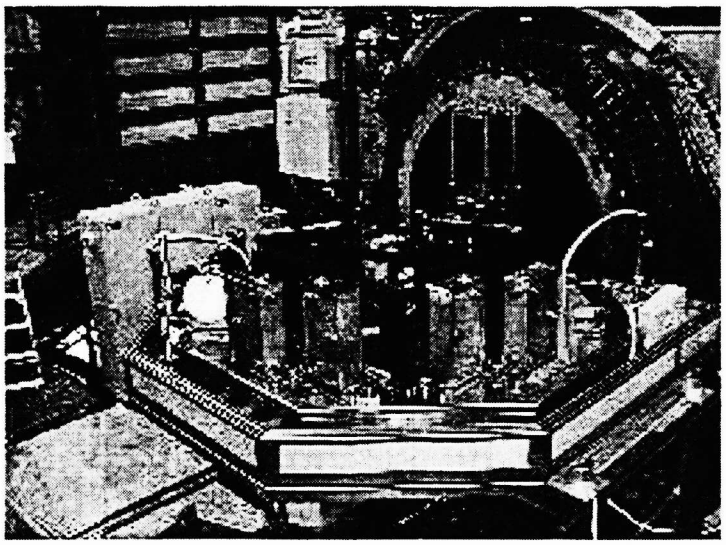

Fig. 1 Picture of UVES taken during commissioning.. The rectangular structures near the table edge are the housings for the off axis parabola mirrirs of the collimator, each is about 50 cm high. The upper half of the enclosure, the blue camera and the red CCD were not mounted at this time.

The field rotation is compensated by an optical derotator. This provides excellent mechanical stability but compared to the Cassegrain, optical losses are larger by about 20% due to the extra reflection on M3 and the need for derotator. However, these losses are compensated by the larger load capacity at Nasmyth which permits a double-beam layout with a good overall efficiency since it allows to optimize coatings, cameras, crossdisperser gratings and CCD detectors for a specific wavelength range.

4. SYSTEM DETAILS

Table and enclosure. The optical functions are located on a ribbed and welded stainless steel table of dimensions 3.2 x 2.8 m and a thickness of 220 mm. The weight of this table and the mounted functions is about 4000 kg. It has it own 3-point adjustable support that is linked directly to the Nasmyth platform.

The 75 mm thick enclosure panels consist of 25 mm Polyurethane panels glued to anodized 2 mm Aluminium panels with an airspace between the PU panels. The panels are supported by a stainless steel frame that is filled with PU foam. The echelle is mounted face-down which helps to keep its surface clean, but has caused some concern about wavelength stability because dispersion is perpendicular to the table. Early thermal studies have shown that external temperature steps of 2° C, for example when opening the dome, can be expected. For this case we have computed thermal gradients across the table of about 0.05° P-V in 12 hours that lead to wavelength shifts on the CCD due to table bending on the order of 20 m/sec/h. With this result we decided to not pursue our original idea of using a customized Invar table. To reduce effects of wind buffeting, the table and enclosure have independent support systems. The upper half of the enclosure weighs about 600 kg and can be lifted by a motorized system in about 2 minutes.

Optical derotator and preslit system. The optical derotator and the calibration lamps are mounted on the rectangular structure of which the top half is visible in Fig. 1 and which is mounted on the telescope adapter. The telescope autoguider will maintain an object stationary with respect to the adapter, so UVES has slitviewers on the red and blue slits to detect and correct any motion that may be due to misalignment of the derotator or movements of the UVES table relative to the adapter. After initial alignment and commissioning such motions were measured to be less than 0.4 arcsec P-V.

The preslit optics relay the F/15 Nasmyth focal plane to the F/10 red and blue slit planes of the spectrograph. Its average efficiency is about 94% (Fig. 5). The diverging F/15 beam from the Nasmyth focal plane enters a fused silica Abbe-Koenig type derotator prism with 3 total internal reflections. To the exit face of this prism a Silica/CaF2 triplet is cemented that collimates the beam. Doublets re-image the Nasmyth focal plane on the slits at F/10 and so allow a more compact instrument by reducing the collimator focal length from 3m to 2m.

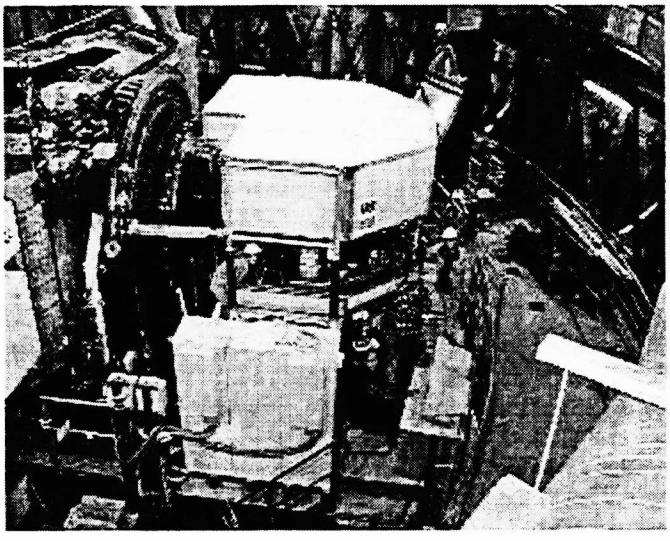

Fig. 2. View of UVES with the enclosure partly open. In the foreground the cooled main control racks and temporary control terminals that were used during the commissioning

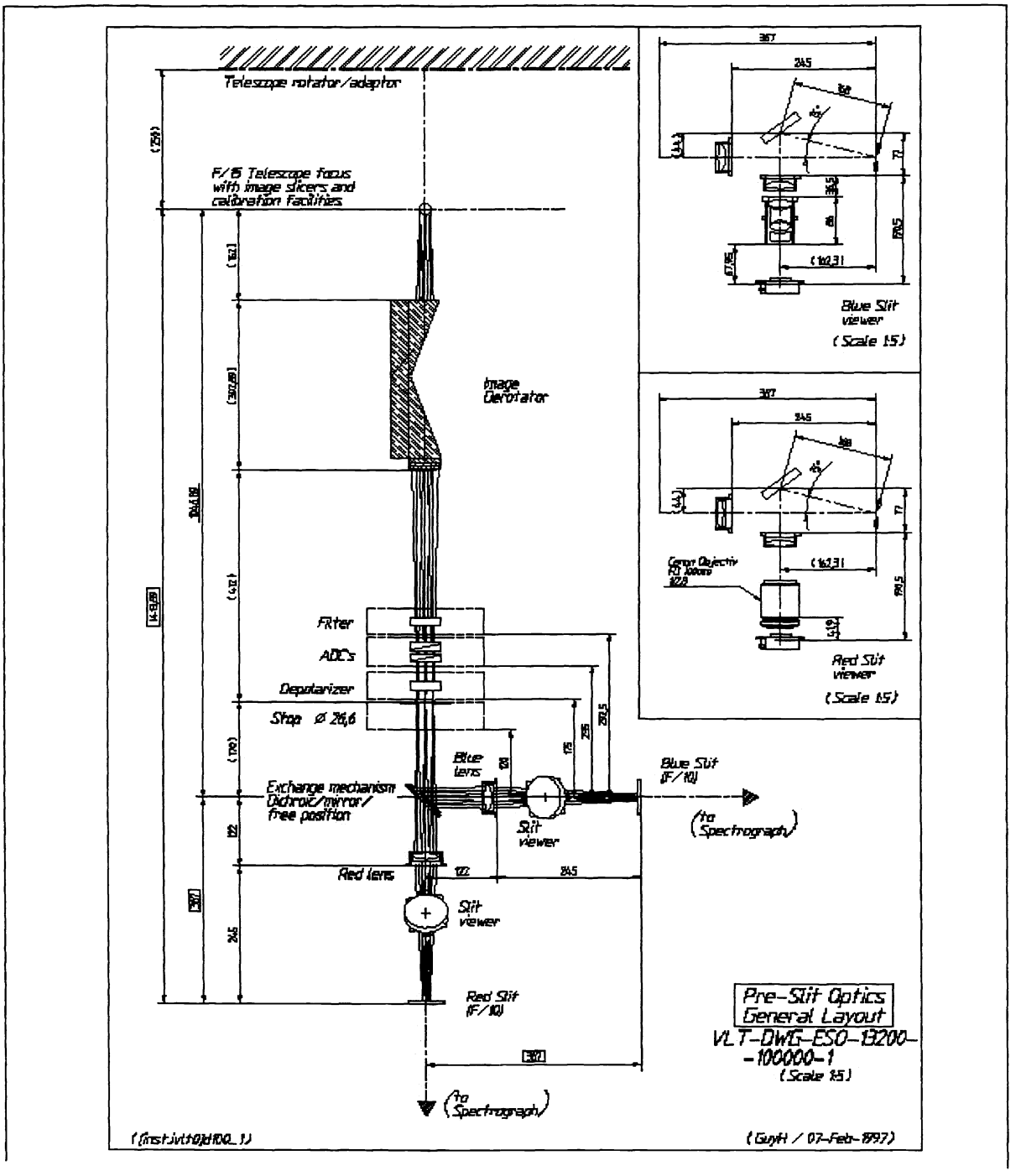

Fig 3 Layout of the preslit optics. This drawing is necessary to understand the operational capabilities of UVES. Before the derotator, a 45° calibration mirror can be inserted, as well as image slicers or an Iodine cell. In the collimated beam behind the derotator at the pupil image of the telescope, a slightly oversized or undersized stray light stop can be inserted. Other options are a filter wheel with a set of UBVRI filters for object acquisition, a rotating superachromatic λ/2 plate to depolarize the light, an ADC that consists of two counterrotating FuSi/CaF2 prisms and a blue mirror or dichroic. The collimated beam is focused on the slits by a red or blue doublet lens. The slit jaws are diamond machined mirrors and Peltier-cooled technical CCDs are used as slit viewers; their sampling is 0.15"/pixel and the limiting V magnitude in good conditions is about 20 for a 3 sec integration. The field of view is 1' of which 30" is unvignetted. The red slit can also be fed by an 8-fiber projector (not shown here) that illuminates the rear of the blue folding mirror.

Calibration lamps. A 45 degree flat calibration mirror can be inserted before the Nasmyth focal plane to direct the light from one of three lamp systems above, to the left or below the derotator. One is a 200 mm Spectralon sphere manufactured by Labsphere equipped with four 30 W external Halogen lamps for flatfielding. Each lamp is dedicated to a restricted wavelength range in which the spectral response is balanced using colour filters (FF2; 380 - 500 nm and FF3; 420 - 700 nm) or by running the lamp at about half the nominal voltage (FF4, 680 - 1000 nm). For test purposes the sphere also has a Mercury lamp and a fiber for injecting light from external light sources like a laser.

The other lamp systems illuminate ground-glass diffusers for higher efficiency. They are a standard Hollow Cathode ThAr lamp for wavelength calibration, and a Deuterium lamp for flatfielding in the 300 - 360 nm region to complement spectra taken with FF lamp 1.

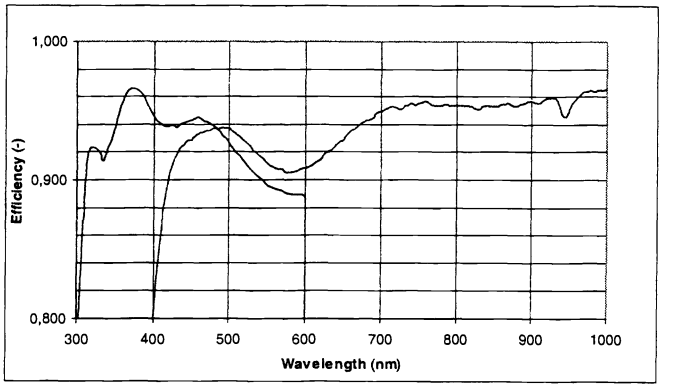

Fig. 5 Measured efficiency of the blue and red preslit optical train up to the slit. All components are A/R coated, the derotator with a wide band A/R coating for 320 - 1000 nm.

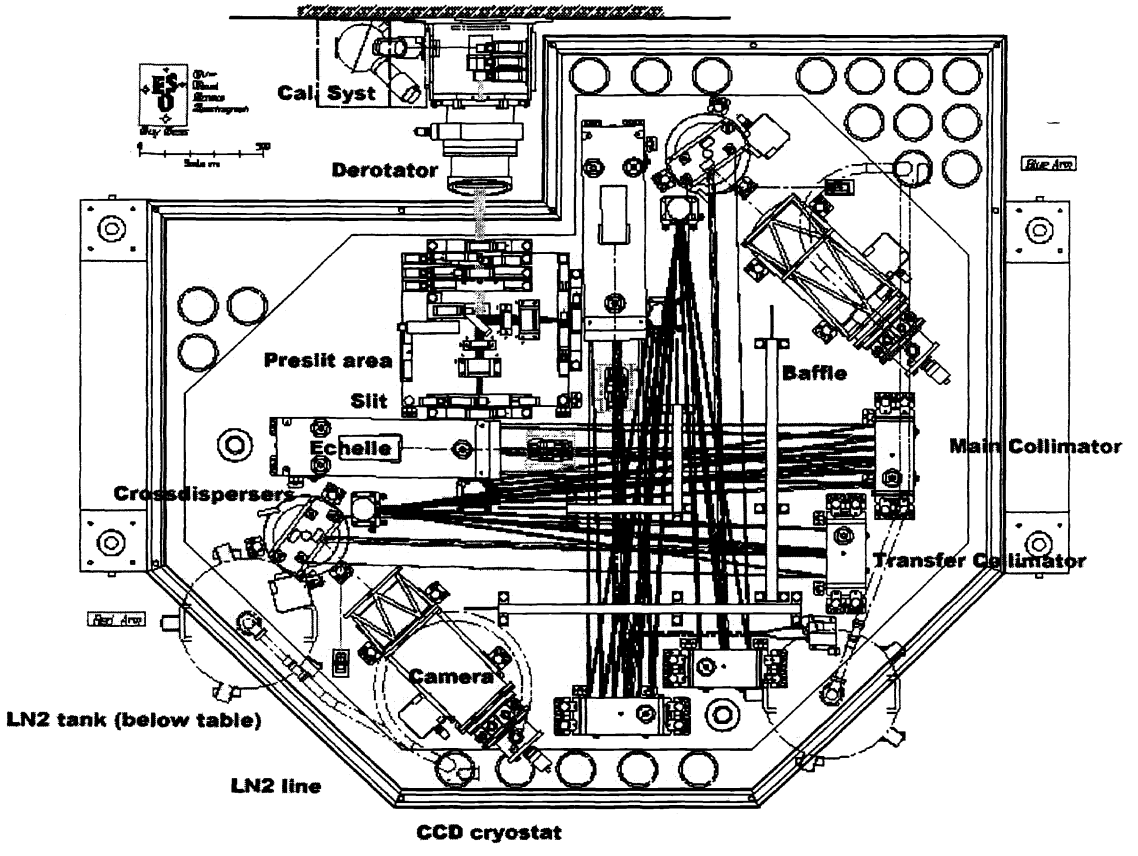

Fig 4 View of the table layout. The main elements of the preslit and of the red spectrograph arm are indicated. The 5-reflection collimators produce a second pupil near the crossdisperser grating and camera to minimize vignetting and are explained in the text. The red and blue arms cross to achieve a compact arrangement. Baffles prevent crosstalk between arms.

Pupil definition is done by the pupil stop behind the derotator, so the lamp and telescope beams match to within 1%. Typical calibration exposure times are on the order of 10^s for a 1" slit and no CCD binning (D_2 lamp 120^s). UVES also has CCD flatfield lamps that are used for engineering tests to monitor CCD read noise, gain and responsivity. The lamps illuminate diffusing screens coated with $BaSO_4$ on the side of the crossdispersers that are rotated to be on the camera axis.

Iodine Cell. A high-temperature Iodine cell can be inserted in the beam before the Nasmyth focal plane. The telescope focus is automatically corrected. The cell imprints on the object spectrum an I_2 absorption spectrum which can be used as a very precise and stable wavelength reference. This technique is described by Marcy and Butler et al. [11,12]. The cell is an evacuated, sealed glass cylinder with a diameter of 74 mm with Pyrex windows of 5 mm and an optical path of 4 cm. We mounted them in an Al housing, isolated by about 1 cm of Al_2O_3 grains and BK7 windows. Evenly distributed strips of heating tape on the cell circumference and windows (except the center) reduce thermal gradients. Full evaporation is reached at 65 °C; the temperature controller maintains the cell at 70±0.3 °C after a 30' warm-up.

Geoff Marcy kindly had three cells built for us that we found to fully evaporate their Iodine at 39, 48 and 65 °C. Marcy had stated he felt that compared to the 35 °C Hamilton and Keck cells, line depth and useful spectral range could be increased by using a higher I_2 column density, and suggested 50 °C for the UVES cell. Our measurements[13] led us to select the 65 °C cell which has on average twice the line depth and a 40% larger useful spectral range compared to the other cell (490 - 640 nm vs. 500 - 610 nm). The Keck and Hamilton cells have a path length of 10 cm and a partial vapour pressure of 0.001 Atm (note that Marcy[11] erroneously quotes the PV pressure of I_2 at 35 °C to be 0.01 Atm). The 65 °C UVES cell has a partial vapour pressure of 0.0078 Atm, so taking into account the 2.5x shorter light path of the UVES cell, the column density is about 3x higher. Together with the resolution of 115 000 of UVES, this cell should provide excellent radial velocity precision. Commissioning data are presently being evaluated.

Image slicers. An advantage of having two conjugate focal planes, is that image slicers or other devices can be inserted in the first F/15 plane without mechanically interfering with the slits in the F/10 plane. The slit has the same width as that of the slicer; and actually defines the slit. Three slicers are mounted on a slide; their characteristics are given in Table 4. All slicers are uncoated. Image acquisition is simple: after initial pointing the acquisition software brings the object on a pre-calibrated position on the slit viewer CCD, after which the slicer is inserted and the derotator placed at the angle that aligns the slicer with the slit. Slicers 1 and 2 have a construction that allows to monitor the sky above and below the slicer (e.g. two times 2" with a 12" decker, depending on the order separation offered by the selected spectral format) while with slicer 3 sky monitoring is not possible. Figure 6 shows a photograph of the 0.44" slicer. This slicer as well as the 0.68" slicer is of the Bowen-Walraven family[14] and consists of a 10 x 4.5 x 4.5 mm, 45° FK5 base prism to which a slicer plate with 45 degree bevels is cemented. The assembly is contacted to a Fused Silica carrier plate and mounted in a cylindrical cell with a Silica cover plate for dust protection. The slicer efficiency is readily measured in the instrument by comparing the exposure meter count rate of a flatfield lamp with the slicer to that with a slit of the same dimensions; we find values of 79, 70 and 60% for slicers 1, 2 and 3, respectively. The losses we attribute to Fresnel losses, slicer imperfections, misalignment between the slicer exit slit and the spectrograph slit, and defocusing effects at the top and bottom of the slicers. In 0.6" seeing we have measured a gain of a factor >3 when moving the 0.3" slicer in front of an 0.3" slit.

Table 4. Image Slicer Parameters

Slicer	*Entrance*	*Slit*	$N_{sclices}$
1	*2.1x2.6"*	*0.68x7.9"*	*3*
2	*1.8x2.0"*	*0.44x7.9"*	*4*
3	*1.5x2.0"*	*0.30x10.0"*	*5*

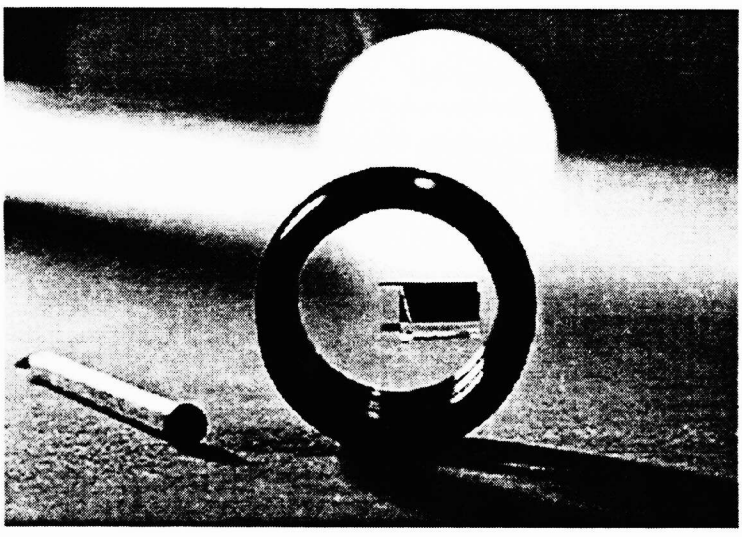

Fig 6 Image slicer no. 2 in its 22 mm cell. The prism is 10 mm long

Slicer no. 3 is a new design that looks like a plane parallel plate of 20x20x6.3 mm. All components are made out of Fused Silica, the

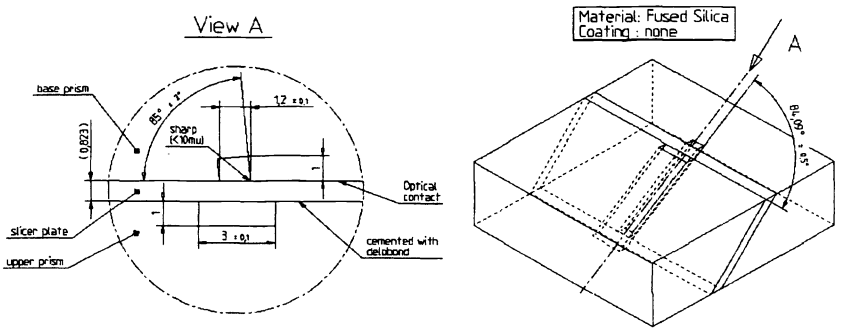

Fig. 7 Construction diagram of the 0.3" image slicer no. 3

angle is 46° to ensure total internal reflection. This concept permits to achieve very narrow slits (Fig. 7) because the fragile slicer plate is well protected during the optical polishing and assembly process. The slicer plate blank is first cemented to the hypotenuse of the top prism in which a 3 mm wide groove has been machined. The width of the grooves is uncritical, while the depth should be large enough to allow cleaning after polishing and cementing. We selected a depth of 1 mm. After cementing the top and bottom faces of the assembly are polished and the slicer plate polished to its final thickness. After cleaning, the bottom prism is contacted to the slicer plate. A 1.2 mm groove is machined in this prism with a sharp "cutting edge" on the side of the groove where the slicing action takes place. The narrow groove has a 6° angle as shown in Fig. 7. This slicer still has potential for improving efficiency by using A/R coatings and micro-etching technology.

Collimator. Below the slits, the light encounters a filter wheel, passes in front of the face-down echelle before hitting a 45 degree folding mirror, and is collimated by the main collimator mirror, an off-axis parabola. The echelle grating operates in Quasi Littrow Mode (QLM); the dispersed beams are again collected by the main collimator and focused (with significant field aberrations) at an intermediate focal plane. A flat folding mirror, which also acts as interorder stray light baffle, directs the light to the pupil transfer collimator that re-collimates the beam and provides a second pupil at the crossdisperser grating. The UVES system was conceived at ESO by B. Delabre. It is a synthesis of the original Baranne "Pupille Blanche" mounting[15] with the Czerny-Turner[16] and Ebert-Fastie grating mountings that also use 2 mirrors in a symmetrical mounting but place the *grating* between the mirrors. This destroys the field symmetry and as a consequence cannot offer coma compensation along the dispersion direction. For an overview see Welford[17]. Our system has been inverted to place the *intermediate focal plane* between the mirrors.

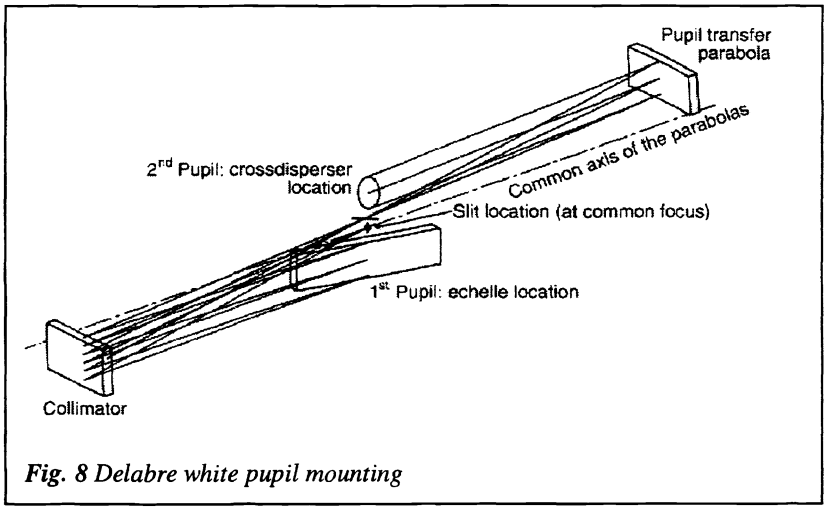

Fig. 8 Delabre white pupil mounting

The UVES arrangement results in perfect aberration compensation of the re-collimated beam except for field curvature which must be corrected by a cylindrical surface near the final image on the detector. The control over the second pupil offered by this type of collimator makes it very well suited to cross dispersed echelle spectrographs as it reduces the oversizing of the crossdisperser and camera compared with to a classical mounting. This advantage was recognized by several groups and the principle has been implemented in several variations in a number of new spectrographs; for instance VELUX at the Nordic Optical Telescope, FOCES at Calar Alto, FEROS at the ESO 1.5m, HRS at the Hobby-Eberly Telescope and SARG at the Italian 3.5m TNG. The only drawback of the arrangement compared to a classical layout with a single reflection on the collimator is that it needs at least 3 reflections while in UVES it was necessary to add 2 flats in order to obtain an accessible slit location and reduce the overall size. By using high-efficiency coatings we could limit the loss per reflection to 3% in the UV-blue, 2% in VIS and 1% in the NIR.

Echelles and crossdispersers It is well known[18,19,20] that the slit limited spectral resolution of a spectrograph is given by $R = \frac{2nd \tan\theta}{D \tan s}$, where R is the resolution, n the index of the medium in which the grating is immersed ($n=1$ in the case of air), d the diameter of the collimated beam on the grating, θ the blaze angle of the grating, D the diameter of the telescope and s the angular slit width. Strictly speaking the equation is valid only for the Littrow case. At an 8 m telescope with a 1" slit, $D.\tan s$ is 40 μm, so the quantity $2nd\tan\theta$ which is the "optical depth" of the grating must be on the order of 1.6 m to reach $R=40\ 000$. Various paths have been followed to achieve these "deep" gratings in current high-resolution spectrograph designs (any combination of big beams, mosaics, high blaze angle and immersion in a medium) see Pilachowski et. al.[1] for a side by side comparison of recent concepts.

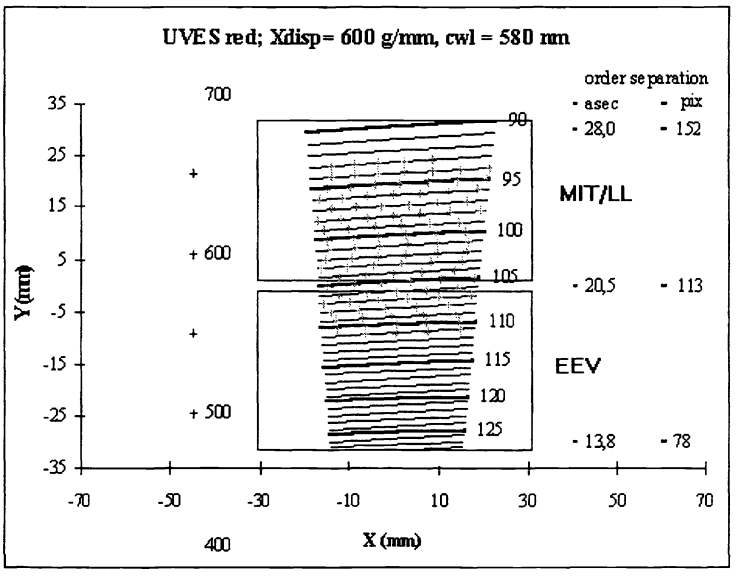

Fig. 9 Spectral format in the red. The length of the plotted orders corresponds to the free spectral range. Almost one full order is lost in the 0.96 mm (64 pixels) gap between the EEV and MIT chips.

The UVES collimator design allows a small off-plane angle (0.8°), much smaller than the typically 5-6° needed to separate incident and diffracted beams in a classical layout. This permitted to use an unusually steep "R4" echelle with a nominal blaze angle of 76° that in the classical case would create difficulties in terms of spectral line curvature, off-Littrow losses and anamorphosis. In UVES the spectral line tilt caused by the off-plane angle is fully corrected by a rotation of the slit by 7 degrees. For $R=40\ 000$ the required beam size is 20 cm. We chose a total length of the grating of 84 cm, matching well a mosaic of two rulings of 408 mm (the greatest length that can be ruled on the B ruling engine of the Richardson Grating Lab) spaced by 14 mm. They are *monolithic* mosaics: two replicas on a single substrate that is simple to mount and has a stable PSF. This concept was validated already in 1992 when RGL delivered a 450x130x70 mm R4 prototype[21,22]. The final echelles were delivered in 1995 and 1996. The echelles are mounted face down in a stationary mount with a multi-point force support to avoid distortion due to gravity. Due to its lower blaze angle, the Rs products of the red echelle is 38 800, while the red echelle delivers the nominal 41 400.

Table 5 UVES gratings and echelles

	ν (g/mm)	blaze	$\lambda\lambda$ (nm)	ε_{blaze}
Blue	*31.6*	*76.0°*	*300-500*	*0.66*
Red	*41.6*	*75.1°*	*420-1100*	*0.70*
CD#1p	*1000*	*430 nm*	*300-390*	*0.63*
CD#2	*660*	*460 nm*	*380-500*	*0.69*
CD#3	*600*	*550 nm*	*420-700*	*0.66*
CD#4p	*312*	*700 nm*	*680-1100*	*0.58*

p: prototype ruling, to be replaced

The need for large order separation did not allow to use efficient prism crossdispersers, so UVES has two red and two blue crossdisperser gratings that are mounted back to back on a turntable. Each grating is optimized for a spectral region with regard to blaze and groove density. The parameters of the UVES gratings are given in Table 5 while Fig. 9 is an example of a red spectral format. CD#1p and #4p are prototype gratings for which replacements are on order. In the case of #1 this is because of a blaze wavelength that lies outside the main operating range of this grating, while #4 has low overall efficiency despite its gold coating. All other gratings are Al-coated.

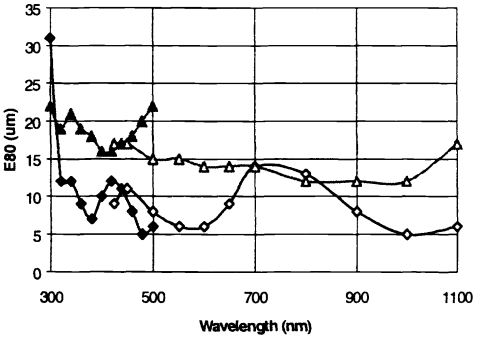

Fig 10. Theoretical image quality of the UVES cameras; axis (lower lines) and field corners (upper lines); T=10°C

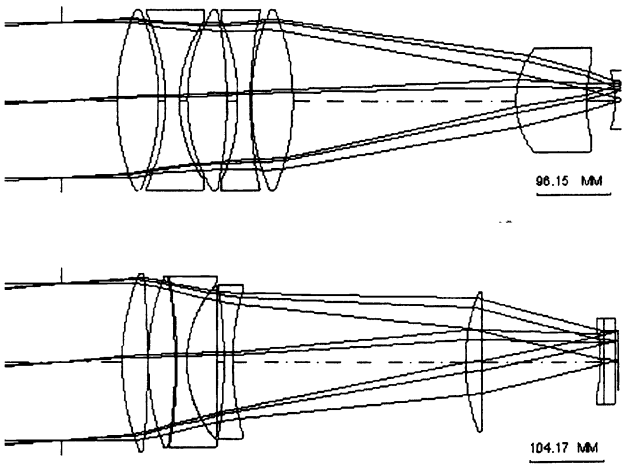

Fig 11 Blue (top) and red (bottom) cameras of UVES. The largest lenses have diameters of 250 mm.

Refractive cameras are used with a measured average transmission of about 85%, no vignetting or central obstruction and an external location of the focal plane that allows interfacing to the standard ESO detector cryostat system. The last camera lens is also the vacuum window. All lenses are multi-layer A/R coated with a typical loss of 1% per surface. The correction of the one dimensional field curvature created by the collimator is achieved by a cylindrical surface on the last surface. The design image quality and layout are given in Figures 10 and 11, the prescriptions after tool and melt adaptation are given in Table 6.

The image quality requirements in the blue can only be achieved with single crystal CaF2, which turned out to be in great demand by suppliers of UV projection lenses for the semiconductor industry. Eventually we managed to obtain 5 blanks from various suppliers.
The blue camera is very sensitive to temperature changes because of the high dn/dT of the glass materials. Focus and spherical aberration are compensated by varying two airspaces by the amounts given in the table. The lens cells are mounted on flexures and moved by passive Al/Carbon Fiber expansion rods. Some light is being generated inside the blue camera, probably by the CaF2, see the section below on CCDs.The red camera requires only one mechanism. Refocusing is automatic and free of play and backlash. To the user, the cameras are fix-focus devices with constant PSF.

The camera designs include 100 mm zero-heat dissipation shutters. The cameras are mounted on tilt tables that allow to move the spectrum in the main dispersion direction by several hundred pixels. This feature was incorporated in the design to move spectral features off bad pixels or mechanical gaps (in case 2K x 2K CCDs would have to be selected). These defects are not present, but this facility might also be used to attain very high S/N using shift-and-add techniques similar to those used in imaging.

The CCDs are EEV CCD-44-82 and MIT CCID-20 2K x 4K devices with 15 μm pixels that in the case of the blue detector is windowed to 2K x 3K. The red detector is a 4K x 4K EEV/MIT mosaic with a gap of 0.96 mm (64 pixels). The Quantum Efficiency as measured in the ESO detector lab is given in Fig. 12. The two-arm, three-chip concept allows to reach a QE envelope that is better than for individual chips. The blue EEV is used from 300 - 500 nm, while in the red EEV has to cover 420 - 860 nm and the MIT is optimized for 680-1050 nm.

TABLE 6 CAMERA CONSTRUCTION DATA (T=20°C)

			Blue			Red
F/Number (nominal)			*1.8*			*2.5*
Spectral Range (nm)			*300-500*			*420-1100*
Clear/nominal dia. (mm)			*210/200*			*220/200*
Focal Length (mm)			*360*			*500*
Field (mm)			*32 x 32*			*62 x 62*
Surf	***Glass***	***Radius***	***Dist***	***Glass***	***Radius***	***Dist***
stop			*70.000*			*83.000*
1	*CaF2*	*300.07*	*53.000*	*FPL51m*	*338.65*	*35.000*
2		*-300.07*	*8.794*		*-*	*1.006*
			+20μm/°		*1383.25*	
3	*Silica*	*-278.27*	*18.000*	*FPL51m*	*338.67*	*37.000*
4		*187.55*	*10.001*		*-744.54*	*2.000*
5	*CaF2*	*229.23*	*50.000*	*KZFSN4m*	*-744.43*	*14.000*
6		*-562.80*	*14.001*	*BK10m*	*169.89*	*41.001*
7	*Silica*	*-265.01*	*16.000*		*18275.0*	*10.000*
					0	
8		*562.80*	*1.003*	*BK10m*	*-744.50*	*12.000*
9	*CaF2*	*300.07*	*53.000*		*370.15*	*323.3*
10		*-300.07*	*286.954*	*SF55m*	*281.82*	*23.000*
11	*Silica*	*109.65*	*90.482*		*infinity*	*165.013*
						+19μm/°
12		*201.77*	*37.265*	*LAH65m*	*-226.46*	*4.000*
			+26μm/°			
13	*Silica*	*-130.99*	*12.000*	*Silica*	*∞*	*17.000*
14 H		*∞*			*∞*	
14 V		*-420.00*	*4.100*		*-420.00*	*4.100*

The measured flatness of the chips inside a cooled dewar is ±16 μm and ±31 μm relative to a flat reference window that was temporarily mounted on the dewar. These numbers include parallelism errors and in the case of the red EEV/MIT mosaic also chip alignment errors.

Although many more modes are technically available, each CCD system is offered with four calibrated readout modes with the most useful combinations of binning and readout clocking rate. We use only one port per chip to simplify calibration and data reduction. Depending on the detector and the chosen combination of binning and readout speed, the read out time is between 30 and 45 seconds and the readout noise is between 3.9 and 1.9 electrons.

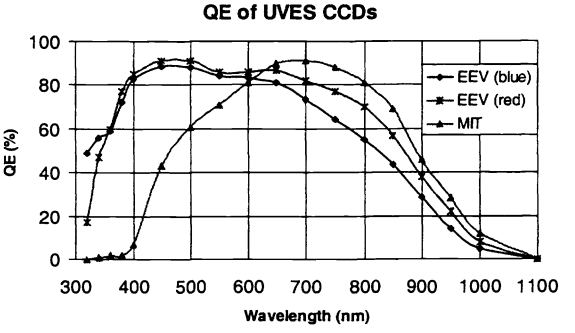

Fig. 12. CCD Quantum Efficiency.

The operating temperature of the chips is -118° C. The CCD cryostats are cooled with a continuous flow of Liquid Nitrogen from 120 L tanks that last typically 10 - 14 days. More information about the UVES CCDs is given in the paper by Dorn et al.[2] and on the UVES web pages.

After waiting 3 - 6 h after startup, all chips reach an intrinsic dark current below 0.5 e/pix/sec,. During commissioning it was noticed that with a cover on the camera, opening the shutter raised the dark current of the blue CCD to 2 e/pix/h. This is probably due to a glow caused by natural radioactivity in CaF2, since in tests on the spare (Russian) CaF2 blank with a PMT (Hamamatsu H4730) we detected a glow of 30 - 50 cps from the blank. In similar tests on materials used inside UVES we were surprised to observe phosphorescence of Zerodur after exposure to strong UV light that took more than 24 h to decay. We decided to paint the optically inactive surfaces of collimator mirrors and gratings black, to reduce the amount of light that can be absorbed by these optics when the UVES enclosure is raised for maintenance.

5. SYSTEM PERFORMANCE

Spectral resolution. One of the products of the data reduction pipeline is an automatic measurement of the FWHM of hundreds of ThAr lines on each CCD chip in the standard blue and red spectral formats. Fig. 14 shows the measured median spectral resolution as a function of slit width, averaged for two CW settings per chip (blue: 342 and 437 nm; red: 580 and 860 nm). The results are consistent with an instrumental LSF of 29, 20 and 27μm for the blue optics + EEV, red optics + EEV and red optics + MIT chips, respectively.

At wide slits, resolution in the blue is a little higher than in the red due to the higher blaze angle of the echelle. At narrow slits the blue resolution suffers from the coarser sampling (0.215 vs. 0.155 "/pix in the red) and currently also from a misalignment in the blue arm. During European system testing the max. spectral resolution in the blue was 90 000.

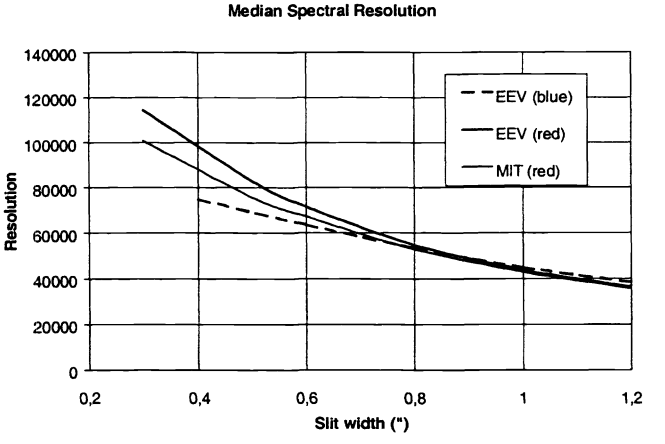

Fig. 14. Median spectral resolution of UVES.

In the red arm, the best resolution is achieved in the part of the spectrum that falls on the EEV chip. This we attribute to a larger charge diffusion in the MIT/LL chip which is also thicker (20 μm) than the EEV (15 μm). Consistent with this is the fact that the degradation is greater in the CW 580 format. At this setting the range 580-680 nm falls on the MIT and so the photoelectrons are generated closer to the back surface of the chip than in the CW 860 format (860 - 1050 nm). It may be possible to reduce charge diffusion in the MIT by adjusting the gate voltages but we this was not done due to lack of time.

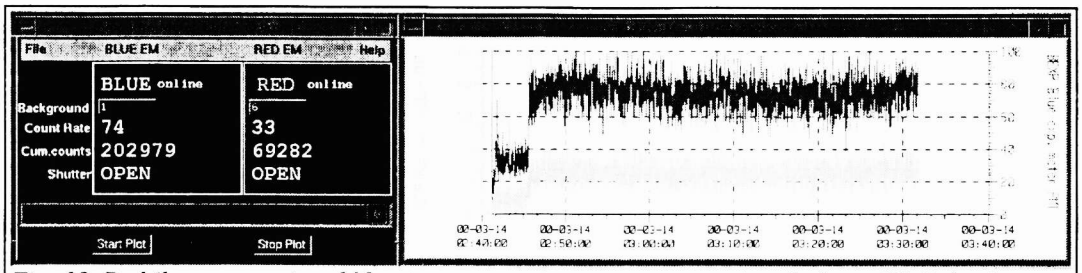

Fig. 13. Red (lower curve) and blue (upper curve) exposure meter signals for a 45' dichroic observation of a blue object with V~18. The exposure was started at t=02:46:00 and at this time the cumulative counters were reset.

Observing efficiency. UVES observations are carried out by the semi-automatic execution of pre-prepared Observing Blocks. For a typical 1 hour exposure with associated ThAr arc spectrum, the observing overheads are 6-8 minutes (depending on how far the telescope must move) for active optics corrections, object acquisition and identification, slit centering and instrument setup. After the integration is finished, 30 - 45 seconds are required for CCD readout (also in dichroic mode) and typically 1 minute for taking the arc spectrum. From these numbers one computes an expected observing efficiency of 85-90%. Slit viewers and exposure meters provide information on the object centering and on the amount of light passing through the slit. As can be seen in Fig. 13, the instantaneous and cumulative number of counts is available to the observer which we found to be very useful during variable observing conditions.

Stability. Since UVES is not pressurized or temperature-stabilized, the position of spectral lines is affected by variations of the refractive index of the air inside the instrument. The sensitivity is 84 m/sec/hPa and -219 m/sec/K at the atmospheric conditions at Paranal. During a night, the internal pressure and temperature change by typically 5hPa and 0.5K, so the apparent radial velocity changes are may be several hundred m/sec. This is the reason why UVES image headers include entries for internal temperature, pressure and humidity. During system testing in Europe we measured an "intrinsic" (i.e. corrected for changes in refractive index of the air) stability and repeatability of 0.03 pixels rms over a 3-day period. At pixel scales of 1560 and 1120 m/sec, this corresponds to 47 m/sec in the blue and 35 m/sec in the red, respectively.

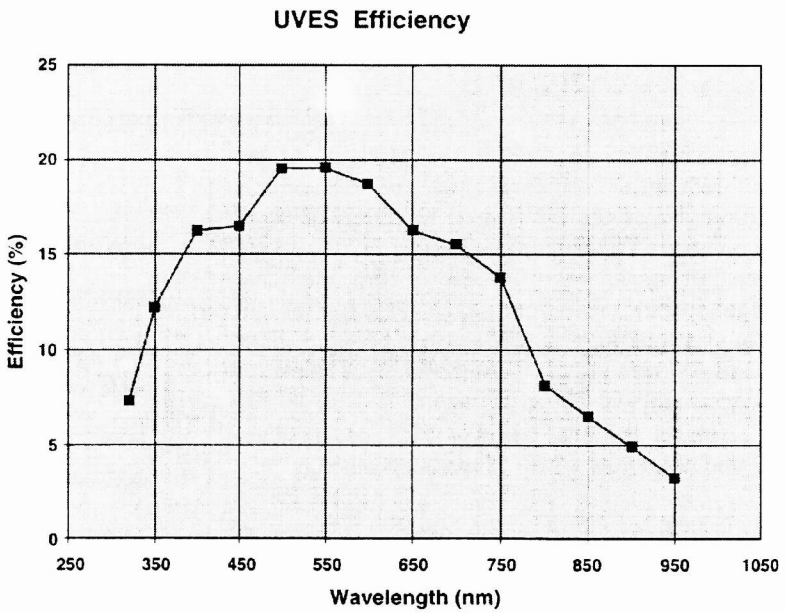

Fig. 15 DQE envelope of UVES as measured from standard star observations in December 1999.

The **Detective Quantum Efficiency** of UVES was measured during commissioning. Figure 15 shows the efficiency envelope that was measured at the center of each order with a wide slit, two dichroics, three CCDs and in four spectral formats. These data were corrected for atmospheric absorption and telescope losses (assumed to be 39% for 3 reflections) and represent the overall instrument DQE (from the entrance focal plane to detected photoelectrons). We expect improvements of 20-30% below 350 nm and above 800 nm when the final crossdispersers will be mounted at the end of the year 2000.

6. THE UVES TEAM

Many people have contributed to UVES. Sandro D'Odorico was the Instrument Scientist. Lex Kaper assisted in writing the Users Manual and the first version of the instrument observing templates. Vanessa Hill helped with the commissioning observations and together with Francesca Primas, Stefano Cristiani and Teasun Kim analysed the first observations. Hans

Dekker was project manager and optical/systems engineer. The mechanics were designed and contracted by Heinz Kotzlowski, assisted by Guy Hess. The electronic control system was designed and built by Serge Moureau with the help of Christian Dietl. The optical designs were made by Bernard Delabre. The Optical Detector team of ESO, headed by Jim Beletic, delivered the UVES CCD systems that were tuned and optimized by Reinhold Dorn with Claudio Cumani for the CCD software. The UVES control and observing software was developed by Antonio Longinotti and Ricardo Schmutzer together with Paulo Santin and Paolo Dimarcantonio at the Astronomical Observatory of Trieste. Jean-Louis Lizon, Christophe Dupuy and Armin Silber were responsible for the optomechanical integration and testing, and for the cryogenics systems. Thanks to Gerd Wieland and Chistine Nieuwenkamp for processing hundreds of purchase orders and to Elena Zuffanelli as department secretary. Paranal Engineering under Peter Gray helped in numerous ways during the commissioning - gracias! Jason Spyromilio was there through all commissioning nights and helped in his special way. Andreas Kaufer developed many of the performance tests and is the operations astronomer of UVES. Pascal Ballester with Stephan Wolf and Andrea Modigliani developed the UVES Exposure Time Calculator and the dedicated data reduction pipeline.

7. REFERENCES

1. C. Pilachowski, H. Dekker, K. Hinkle, R. Tull, S. Vogt, D.D. Walker, F. Diego and R. Angel, "High-Resolution Spectrographs for Large Telescopes", *PASP 107, 983-989,* 1995
2. R. Dorn, C. Cavadore, J. Beletic, J.L. Lizon, "Design, construction, and operating parameters of the CCD systems for the blue and red arms of UVES: the Echelle Spectrograph for the UT2 Kuyen Telescope at the ESO Paranal Observatory", *Proc. SPIE 4008 (in print)*, 2000
3. A. Longinotti, P. Dimarcantonio and P. Santin, "UVES Instrument Software in the VLT Environment", *Proc. SPIE 4009 (in print),* 2000
4. Ballester , P. Grosbol, K. Banse, A. Disaro, D. Dorigo, A. Modigliani, J.A. Pizarro De La Iglesia, O. Boitquin, "Quality Control System for the Very large Telescope", *Proc. SPIE 4010 (in print)*, 2000
5. S. D`Odorico and L. Kaper , "UVES User Manual Issue 1.0", *http://www.eso.org/instruments/uves/userman/*
6. A. Kaufer, "UVES, the VLT UV-Visual Echelle Spectrograph", *http://www.eso.org/instruments/uves/*
7. S. D'Odorico, "Scientific Capabilities of UVES, the Echelle spectrograph at the VLT and highlights of the first observations of stars, galaxies and QSOs", *Proc. SPIE 4005 (in print)*, 2000
8. H. Dekker and S. D'Odorico, "UV-Visual Echelle Spectrographs (UVES1 and UVES2) Design and Implementation Plan", *ESO Scientific and Technical Committee doc. no. 130*, 1992
9. H. Dekker and S. D'Odorico, "UVES Upgraded Design and Implementation Plan", *ESO Scientific and Technical Committee doc. no. 151*, 1994
10. L. Pasquini, "FLAMES, a multiobject fiber facility for the VLT", *Proc. SPIE 4008 (in print)*, 2000
11. G. Marcy and P. Butler, "Precision Radial Velocities with an Iodine Absorption Cell", *PASP 104, pp. 270-277*, 1992
12. P. Butler, G. Marcy, E. Williams, C. McCarthy, P. Dosanh and S. Vogt, "Attaining Doppler Precision of 3 m/sec", *PASP 108, 500-509*, 1996
13. M. Kuerstner, "Properties of the UVES Iodine Cells #1 and #2", *ESO internal report* (1999)
14. Th. Walraven and J.H. Walraven, "Some Features of the Leiden Radial Velocity Instrument", *Proc. ESO/CERN Conf. on Auxiliary Instrumentation for Large Telescopes, eds. S. Lautsen and A. Reiz*, pp. 175 - 183, 1972
15. A. Baranne, "Equipement Spectrographique du Foyer Coude du Telescope de 3,60 metres", *Proc. ESO/CERN Conf. on Auxiliary Instrumentation for Large Telescopes, eds. S. Lautsen and A. Reiz, pp. 227-239*, 1972
16. M. Czerny and A.F. Turner, *Zeits. f. Physik 61, p. 590,* 1930
17. W.T. Welford, "Aberration Theory of Gratings and Grating Mountings", *Progress in Optics IV, ed E. Wolf, p. 264,* 1965.
18. D. Hall, "Matching High Resolution Grating Spectrographs to Large Telescopes", *KPNO Conf. on Optical and Infrared telescopes for the 1990s, ed. A. Hewitt, pp. 336-341*, 1980
19. H. Dekker, "An Immersion Grating for an Astronomical Spectrograph", in *Proc. 9th Santa Cruz Summer Workshop on Instrumentation for Ground-based Astronomy, ed. L.B. Robinson, pp.183-188,* 1987
20. R. Szumski and D. D. Walker, "The Immersed Echelle I. - Basic Properties", *MNRAS 302, pp. 139-144,* 1999
21. H. Dekker and S. D'Odorico, "UVES, the UV-Visual Spectrograph for the VLT", *The Messenger 70, pp. 13-17*, 1992
22. H. Dekker and J. Hoose, "Very High Blaze Angle (R4) Echelle Mosaic", in *ESO Workshop on High Resolution Spectroscopy with the VLT, ed. M. -H. Ulrich, pp. 261-266*, 1992